

Universidade de São Paulo
Faculdade de Filosofia, Ciências e Letras de Ribeirão Preto
Departamento de Computação e Matemática

Comparing the LMC Complexity of Neural Networks with their Inference Capability

Author: Lucas Miranda Mendonça Rezende
Supervisor: Ph.D. Luiz Otavio Murta Junior

November 4, 2025

Abstract

TO DO

Contents

1	Introduction	3
1.1	Work thesis	4
1.2	Objective	4
2	Methodology	5
2.1	Testing Environment	5
2.2	Model Selection	6
2.3	LMC Complexity	7
2.3.1	Reading Model Weights	8
2.3.2	Filtering	9
2.3.3	Data Discretization and Histogram	10
2.3.4	Complexity Calculation	11
2.4	Inference Capability	11
2.4.1	Benchmark Selection	11
2.4.2	Benchmark Collection Procedure	13
2.5	Comparing LMC Complexity and Inference Capability	14
2.5.1	Building the testing dataset	14
2.5.2	Regression procedures	16
2.5.3	Influence of filtering	17
2.5.4	Influence of weight types	17
2.5.5	Complexity vs Number of parameters	18
2.5.6	Complexity vs Number of bins	18
2.5.7	Complexity vs Benchmark performance	18
3	Results	20
3.1	Extraction process	20
3.2	Filter dimension	20
3.3	Weight-type dimension	25
3.4	Complexity vs Number of parameters	27
3.5	Complexity vs Number of bins	27
3.6	Complexity vs Benchmarks	28

1 Introduction

Since the creation of Transformers in 2017 [1] and the subsequent usage of this new technique in the training of Large Language Models (LLMs), there has been a gold rush within the machine learning world. GPT-3.5, the original ChatGPT model, rapidly gained widespread adoption, becoming the fastest-growing consumer application in history after its launch in 2022 [2], sparking further interest in researchers, investors, and the general public for more powerful and cost-efficient models.

Since then, multiple new models have been developed by the biggest technology companies in the world such as Google, Microsoft, NVIDIA, Amazon, and amazingly also by some smaller ones such as DeepSeek. As better models in almost every metric emerged, it also became increasingly obvious that all this improvement was not for free: billions were spent in larger datacenters, predictions that we soon would not have enough data on the internet to keep building bigger models, increasingly expensive for marginal performance gains. But why?

In 2020, before the launch of the original ChatGPT, researchers at OpenAI [3] found that "performance improves smoothly as we increase the model size N (the number of parameters excluding embeddings), dataset size D , and amount of compute C " and that "performance depends strongly on scale and weakly on model shape, such as depth vs. width". Second, it was also observed that different architectures could impact training performance, e.g., Transformers would have lower test loss than LSTMs. Those statements became the basis for the scaling "laws" we currently accept.

It is evident that the most straightforward way to get a better model, at least considering performance in terms of lower test loss, is to increase the scale (N , C , and D sizes). However, there is a huge drawback: the scaling laws described in this case are power laws, meaning we would need an exponential amount of resources to achieve a constant gain in performance. The second approach would be creating better architectures or improving the existing ones, which demands research and is generally not as simple as increasing a number.

The first approach, being the easiest, was explored by the companies creating the new models, pushing those three variables to ludicrous amounts. The GPT family, mentioned above, serves as a good example: the original GPT had 117 million parameters, GPT-2 had 1.5 billion (a 12x increase from GPT), and GPT-3 had 175 billion (a 117x increase from GPT-2) [4] [5] [6]. It is noticeable that, just a few years later, the industry is already showing signs of exhaustion: new models do not exhibit performance improvements as dramatic as those observed in the recent past, although investment in training infrastructure has never been higher.

The second approach is what we intend to contribute in this work: an improve-

ment in the architecture itself. Of course, before creating a new revolutionary architecture it would be useful to understand how machines learn. In a typical analysis setting, knowing how the process works is a requirement to engineer a better version of it. In Machine Learning, however, the process of learning, which is somehow connected to the well-known process of training, is still far from being fully understood.

Discussing the understanding of the learning process is out of the scope of this work. Yet, we are going to analyze what may be a piece of the puzzle: the LMC statistical complexity [7], a metric that appears to be related to the model's performance and might help in understanding the behavior of such by providing insights about the weights distribution.

1.1 Work thesis

The main hypothesis of this work comes from Professor Luiz Otavio Murta Junior [8] and can be summarized as: **"There exists a relationship between model complexity and its inference capability"**.

1.2 Objective

Validating the work thesis means we would have a new way of indirectly assessing a model's performance by just looking at the distribution of its weights, opening the door to new optimization processes during training, potentially reducing the amount of compute necessary to reach the best performance or even discovering new maxima. Also, having a validated weights distribution vs. performance comparison should improve the data richness when studying a model's learning process in future studies. Thus, we can establish the following objectives for this work:

- Validate the existence of a meaningful relationship between complexity of neural network weights and their inference performance.
- If possible, find the mathematical relation between those measures.
- Explore other dimensions of the problem that can affect complexity and performance measures such as parameter count.

2 Methodology

2.1 Testing Environment

We used the following computational environment for our experiments:

- OS: Linux 6.8.0-64-generic
- CPU: 2x Intel Xeon Gold 6130 @ 2.1GHz - 32 cores / 64 threads per CPU, 22M cache each
- RAM: 512GB DIMM 2400 MHz (DDR4)
- GPU: NVIDIA Quadro P5000 (GP104GL) - 16GB VRAM
- Storage: RAID5 (2x4TB) 8TB SAS with Broadcom MR9260-8i controller + 512GB RAID0 SSD

The hardware was provided for research purposes by Universidade de São Paulo. The choice of this environment was motivated by the availability of a high-performance GPU and large quantities of RAM necessary for handling large language models.

We used the following tools and libraries:

- Python 3.12.3
- PyTorch 2.8.0 [9]
- Transformers 4.56.2 [10]
- Hugging Face Hub 0.35.0 [11]
- Numpy 2.2.6
- Pandas 2.3.2
- Pysr 1.5.9
- SciPy 1.16.1 [12]
- Matplotlib 3.10.6
- Seaborn 0.13.2 [13]
- CUDA Toolkit 12.6

The choice of versions was motivated by compatibility with our computational environment GPU.

2.2 Model Selection

Due to the wide availability of open models combined with the ease of accessing them through the Transformers library [10] and Hub library [11], **Hugging Face** was chosen as the source for model selection in this study.

Hugging Face is a platform that hosts a variety of machine learning models, datasets, and tools. It is widely used in the AI research community for sharing and collaborating on machine learning projects [14, 15]. Other platforms such as Ollama [16] were considered, but ultimately not chosen due to the limited number of models available and fewer contributing companies.

Model selection proceeded in two stages:

1. First, we identified major technology companies by market capitalization that publish openly released language models. The companies considered were **OpenAI**, **Google**, **Meta**, and **Microsoft**.
2. Second, for each company we compiled a candidate set consisting of every model that satisfied the following criteria:
 - Must be available on the Hugging Face platform on the official company account.
 - The model is a transformer-based language model.
 - Model weights are publicly accessible (open weights), including models released behind gated access.
 - The model is text-only (no multimodal image/audio inputs).
 - The model is an original base model rather than a task-specific fine-tuned variant.
 - The total parameter count is below 150 billion. This upper bound was imposed due to hardware and inference limitations in the computational environment used for our experiments.
 - The model is supported by the Hugging Face Transformers library [10] (i.e., it can be instantiated via the AutoModel utility), which ensures consistent loading and preprocessing across the candidate set.
 - There is at least one publicly available benchmark result for the model among the selected benchmarks (section 2.4.1).

The final selection of models used in this study is listed in Table 1.

Meta	Google	Microsoft	OpenAI
meta-llama/Llama-4-Scout-17B-16E	google/gemma-3-27b-pt	microsoft/Phi-4-mini-reasoning	openai/gpt-oss-120b
meta-llama/Llama-3.2-3B	google/gemma-3-12b-pt	microsoft/Phi-4-reasoning	openai/gpt-oss-20b
meta-llama/Llama-3.2-1B	google/gemma-3-4b-pt	microsoft/Phi-4-reasoning-plus	openai-community/gpt2-xl
meta-llama/Llama-3.1-70B	google/gemma-3-1b-pt	microsoft/phi-4	openai-community/gpt2-large
meta-llama/Llama-3.1-8B	google/gemma-3-270m	microsoft/phi-2	openai-community/gpt2-medium
meta-llama/Meta-Llama-3-70B	google/gemma-2-27b	microsoft/phi-1_5	openai-community/gpt2
meta-llama/Meta-Llama-3-8B	google/gemma-2-9b	microsoft/phi-1	
meta-llama/Llama-2-70b-hf	google/gemma-2-2b		
meta-llama/Llama-2-13b-hf	google/gemma-7b		
meta-llama/Llama-2-7b-hf	google/gemma-2b google/recurrentgemma-9b google/recurrentgemma-2b		

Table 1: Selected language models included in this study.

Meta Models: [17] [18] [19] [20] [21] [22] [23] [24] [25] [26]

Google Models: [27] [28] [29] [30] [31] [32] [33] [34] [35] [36] [37]

Microsoft Models: [38] [39] [40] [41] [42] [43] [44]

OpenAI Models: [45] [46] [47] [48] [49] [50]

2.3 LMC Complexity

According to [7], LMC Statistical Complexity is the product of two other measures: Disequilibrium and Shannon entropy. It captures both the structured and

unstructured aspects of the distribution:

$$C_{LMC} = H \times D$$

Disequilibrium measures how far a probability distribution is from being uniform, quantifying the "order" or structure in the data. It is calculated as:

$$D = \sum_{i=1}^n \left(p_i - \frac{1}{n} \right)^2$$

Shannon entropy measures the amount of uncertainty or randomness in a probability distribution. The normalized Shannon entropy is given by:

$$H = -K \sum_{i=1}^n p_i \log p_i$$

The values p_i represent the probabilities associated with each state i in the distribution, and n is the total number of states. K is a positive constant and, in our case, is set to 1 for simplicity. K can be changed later since $C_{LMC} = (-K \sum_{i=1}^n p_i \log p_i) \times D$ is equivalent to $C_{LMC} = K \times (-\sum_{i=1}^n p_i \log p_i) \times D$.

2.3.1 Reading Model Weights

Model weights are fetched using the Hugging Face Hub library [11] and loaded using the Transformers library [10]. For each selected model, we instantiate the model using the **AutoModel** utility, which automatically handles model architecture loading and weight initialization.

The models are loaded entirely into the main memory instead of a GPU since the amount of VRAM available in the computational environment is insufficient for larger models (> 70 billion parameters). Other problems such as handling symbolic tensors also motivated this decision.

Using the main memory is considerably slower than using a GPU, but allows us to work with larger models without running into memory limitations. Since we had a large amount of RAM, we decided to cast all the model weights to float32 during the AutoModel instantiation as CPUs generally handle this format natively and, as a consequence, make calculations faster.

Once loaded, we extract all the parameters from the model using the `named_parameter()` method provided by the Transformers library. This method returns an iterator over all model parameters, each parameter being represented as a tensor.

We then flatten each tensor into a one-dimensional array and store it in a list. Each array is labeled in one of the following **weight-type categories**:

- Bias: if 'bias' is in the parameter name
- Norm: if 'norm' is in the parameter name
- Embedding: if 'embed' is in the parameter name
- Other: all other weights

These categories are the most common types of weights found in this architecture and will be used later as another dimension of analysis.

The choice of also analyzing by weight type is motivated by the fact that different weight types may exhibit different statistical properties and, as a consequence, different complexity characteristics. Studies such as the already cited OpenAI's [3] take into account different weight types when analyzing scaling laws.

2.3.2 Filtering

Casting different encoding formats to float32 may introduce rounding errors that manifest as extreme outliers in the weight distribution. This is rare (approximately 10 to 30 values in 100 billion) but can be problematic for our next step: histogram construction (section 2.3.3), since the number of bins will be affected by the range of values in the data. The reasons for those rounding errors could not be fully investigated within the scope of this work, but they are likely related to floating point rounding errors.

To mitigate the impact of outliers, we will apply a value removal approach. This process filters the data to retain only values within a configurable range centered around the mean:

$$\text{lower bound} = \mu - \sigma_{\text{filter}} \cdot \sigma$$

$$\text{upper bound} = \mu + \sigma_{\text{filter}} \cdot \sigma$$

where μ is the data mean, σ is the data standard deviation, and σ_{filter} is a configurable parameter that controls the filtering strength. Values falling outside this range are excluded from further analysis.

It is not trivial to choose the best value for σ_{filter} . A very low value may remove important parts of the distribution, while a very high value may not effectively mitigate the outlier problem. For this reason, we will experiment with different values of σ_{filter} and analyze how they affect the final complexity results. As a consequence, this becomes yet another dimension of analysis in our study.

The values of σ_{filter} tested will be: **0.125, 0.25, 0.5, 1, 2, 3, 4, 5, 10, 20**. The choice of σ_{filter} that will be used as the data's filtering option for the next steps is the one that:

1. most reduces the bin count compared to the unfiltered data;
2. has the least amount of filtering or, in other words, the highest value of σ_{filter} among the ones chosen in the first criterion.

2.3.3 Data Discretization and Histogram

To compute the LMC complexity of a finite array of floating-point numbers, we first construct a histogram to discretize the data into a probability distribution. This is justified as the chance of finding two exact numbers is extremely low and, as a consequence, it is hard to determine the probability of each value.

We will call the set of all data points as S , the total amount of data points as N and the number of bins they will be distributed into as n . The probabilities p_i are then calculated as $p_i = \frac{f_i}{N}$ where f_i is the frequency count of data points in bin i .

As expected, this approach revisits a classic issue in histogram-based analysis: the choice of the number of bins n will impact the resulting probability distribution, which is particularly problematic for the LMC complexity measure; variations in n can cause significant fluctuations in the final result. Selecting an inappropriate amount may produce misleading values, either by oversimplifying the distribution (too few bins) or by introducing noise (too many bins).

There are a variety of methods to determine n in a histogram, most of them with their own advantages and disadvantages. Commonly used methods such as **Sturges' formula** [51] and **Rice Rule** [52] rely only on the number of data points, while others like **Scott's normal reference rule** and **Freedman-Diaconis' choice** also take into account the data distribution by using standard deviation and interquartile range, respectively [53].

We chose to use the **Freedman-Diaconis' choice** as it adapts better to our needs. This is justified since N often consists of billions of numbers, and the distribution, although mostly concentrated between -1 and 1, can become sparse due to outliers and, as a consequence, require a larger number of bins to capture its characteristics accurately. The Freedman-Diaconis rule helps mitigate the influence of outliers by using the interquartile range IQR to determine bin width h . The rule is defined as follows [54]:

$$h = \frac{2 \times IQR}{N^{1/3}}$$

where IQR is the interquartile range of the data which is calculated as $Q3 - Q1$, $Q3$ and $Q1$ are the values at the 75th and 25th percentiles in the data, respectively. Since N is very large, the percentiles are computed based on a random sample of

100000 data points to reduce computational cost. The sample size was determined empirically to be large enough to provide stable estimates of the percentiles, the final number of bins showed no variance between tests.

The number of bins n can then be calculated as:

$$n = \frac{\max(S) - \min(S)}{h}$$

Finally, we can use the already filtered data and the calculated n to build a histogram using a simple function provided by PyTorch [9]. Then, compute the probabilities p_i for each bin i .

2.3.4 Complexity Calculation

With the probabilities p_i computed from the histogram, we can now calculate the LMC complexity C_{LMC} using the formulas provided in the beginning of section 2.3. This involves calculating the Disequilibrium D and the Shannon entropy H using the probabilities, and then multiplying them to obtain the final complexity measure C_{LMC} .

2.4 Inference Capability

Often called model performance, inference capability refers to how well a trained neural network performs on unseen data. This is typically measured using various metrics depending on the specific task the model is designed for.

In the previously cited research paper by OpenAI [3], performance was associated with test cross-entropy loss. This metric quantifies the difference between the predicted probability distribution output by the model and the true distribution of the target labels. Lower cross-entropy loss values indicate better model performance, as they reflect a closer alignment between predictions and actual outcomes.

Unfortunately, not all models we intend to analyze have publicly available training and test data. It's also not possible to run models in a training setting due to performance limitations of the computational environment available. Therefore, we will have to rely on imperfect proxies for performance such as **benchmarks**.

2.4.1 Benchmark Selection

Benchmarks are standardized tests designed to evaluate the performance of machine learning models across various tasks. They provide a common ground for

comparison by measuring how well different models perform on the same datasets using predefined metrics.

According to [55], benchmarks such as the famous MMLU, correlate fairly well with the predicted test loss determined by scaling laws, making them suitable proxies.

They are, however, not perfect. Some benchmarks may fail to capture all aspects of a model’s capabilities, leading to an incomplete assessment of performance. Other problems such as Data Contamination [56] can influence the validity of results and make it difficult to fairly compare models created at different times. It is also hard to find benchmarks that are widely reported for all models we intend to analyze.

A nice proposal for future research to avoid the problems cited above would involve training a model from scratch twice: optimizing it initially for minimal loss and then for minimal loss + maximum LMC complexity, then comparing the results. This is however out of the scope of this work.

The benchmark selection followed three main heuristics:

- **Relevance:** The benchmark should be widely recognized and accepted in the machine learning community, e.g., used in major research papers.
- **Generality:** It should cover a range of tasks and data types to provide an assessment of model performance across different scenarios, that is, not being specialized in one task.
- **Availability:** The benchmark results should be publicly available. Benchmarks that cover more of the selected models were preferred.

Based on those heuristics, the benchmarks selected were:

- **MMLU (5-shot):** Massive Multitask Language Understanding, a benchmark that tests models across 57 tasks spanning various subjects and difficulty levels. Widely used to evaluate LLMs [57].
- **MMLU-Pro (5-shot):** An enhanced version of MMLU that includes additional tasks and updated datasets to provide a better evaluation [58].
- **OpenLLM (Average):** A benchmark suite that evaluates models on a variety of tasks, including language understanding, generation, and reasoning. It aggregates results from multiple datasets to provide an overall performance score [59].
- **LMArena (Score):** An online platform where users can submit questions and receive responses from two anonymous large language models (LLMs),

then vote on which answer they prefer, helping to crowdsource human preferences for evaluating and ranking LLMs. Its evaluation works by collecting thousands of pairwise comparisons from users, using the Bradley-Terry system to estimate win rates and compute rankings/scores. [60].

2.4.2 Benchmark Collection Procedure

Benchmark values were manually collected from multiple sources, in the following order of priority:

1. Official *Hugging Face* model pages
2. Original research papers
3. Official websites
4. Third-party websites

Meta Models: [17], [18], [19], [20], [21], [22], [23], [24], [25], [26]

Google Models: [27], [28], [29], [30], [31], [32], [33], [34], [35], [36], [37]

Microsoft Models: [38], [39], [40], [41], [42], [43], [44], [61], [62]

OpenAI Models: [45], [46], [47], [48], [49], [50], [63],

Additional References: [15], [16], [64], [65],

If more than one source was available for the same model and benchmark, the one with higher priority was chosen. Not all models had results available for all benchmarks. Figure 1 shows the availability matrix.



Figure 1: Availability of benchmark results for the selected models.

2.5 Comparing LMC Complexity and Inference Capability

2.5.1 Building the testing dataset

We will build a dataset by creating tuples that encode all dimensions of our analysis: model information, weight-type combination, filtering setting, the resulting LMC complexity value, the number of histogram bins used, and the available benchmark results for the model.

The dataset construction follows a nested loop structure:

1. **For each model** in our selected set (e.g., Llama-4-Scout-17B-16E, gpt-oss-120b, etc.), we generate all non-empty subsets of the four **weight-type categories** defined in section 2.3.1 using the power set [66]. This produces 15 unique weight-type combinations per model:

- Single types: {bias}, {norm}, {embedding}, {other}
 - Dual combinations: {bias, norm}, {bias, embedding}, {bias, other}, {norm, embedding}, {norm, other}, {embedding, other}
 - Triple combinations: {bias, norm, embedding}, {bias, norm, other}, {bias, embedding, other}, {norm, embedding, other}
 - All four: {bias, norm, embedding, other}
2. **For each weight-type combination**, we apply every value of σ_{filter} defined in section 2.3.2. The filtering values tested are: 0.125, 0.25, 0.5, 1, 2, 3, 4, 5, 10, 20, plus one unfiltered configuration, totaling 11 configurations per combination.
 3. **For each configuration**, we compute the LMC complexity following the procedure outlined in section 2.3. We also record the number of histogram bins used in the calculation for further analysis. Lastly, we append the available benchmark results for the model from section 2.4.2.

At the end we will have $35 \text{ models} \times 15 \text{ weight-type combinations} \times 11 \text{ filtering settings (including unfiltered)} = 5775 \text{ datapoints}$. The resulting dataset **R** consists of tuples structured as follows:

1. Model name
2. Number of parameters
3. Weight-type combination
4. Filtering setting
5. LMC complexity value
6. Number of histogram bins
7. Available benchmark results

e.g. a hypothetical tuple in the dataset:

- (Llama-4-Scout-17B-16E, 17B params, {bias}, 0.125, 0.324, 8592, [MMLU: 71.2, MMLU-Pro: 68.5, ...])

2.5.2 Regression procedures

We will also use two important concepts defined as follows:

- **Linear regression:** a conventional statistical method used to model the relationship between a dependent variable and one or more independent variables by fitting a linear equation [67]. The data may not follow a linear trend, but linear regression can still be used to identify overall correlations and make it easier to compare results.

- Linear: $y = ax + b$

For comparisons, we will use the **Pearson correlation** [67] (linear correlation coefficient). This can be computed as:

$$r = \frac{\text{cov}(x, y)}{SD(x) \times SD(y)}$$

where $\text{cov}(x, y) = (\text{average of products } xy) - (\text{average of } x) \times (\text{average of } y)$.

Or alternatively, using the linear regression slope a [68]:

$$r = a \cdot \frac{SD(x)}{SD(y)}$$

- **Free regression:** a curve fitting method with greater flexibility but less comparability than linear regression. It was configured to test for the following functions:

- Linear: $y = ax + b$
 - Quadratic: $y = ax^2 + bx + c$
 - Exponential: $y = a \cdot e^{bx} + c$
 - Logarithmic: $y = a \cdot \ln(x + 1) + bx + c$
 - Power: $y = a \cdot (x + 1)^b + c$

The best fit was chosen based on the highest R^2 value.

For both regressions, the tests were made using `curve_fit` from SciPy [12].

2.5.3 Influence of filtering

In more detail, the criteria defined in section 2.3.2 to choose the best filtering setting works as follows:

1. We will group R in relation to each value of σ_{filter} . Then, calculate the **average** and the **maximum histogram bin count** for each group, and plot them as a bar chart.
2. We will group R in relation to each value of σ_{filter} . Then, calculate the **average** and the **maximum complexity** for each group, and plot them as a bar chart.
3. Since steps 1 and 2 represent the two criteria defined in section 2.3.2, we will first filter the groups obtained in 1 to keep only the ones that have a lower average bin count than the unfiltered data. Then, among those groups, we will choose the one with the closest complexity value to the unfiltered data (least amount of filtering).

The filtering dimension will be used to determine the best general filtering setting following the criteria defined in section 2.3.2. After defining the best filtering setting, we will discard all the runs where σ_{filter} is different from the chosen one, creating a new set \mathbf{R}_{best} . There will be a total of: 35 models \times 15 weight-type combinations \times 1 filtering setting = 525 datapoints.

We will also make a free regression on a scatter plot for the data obtained in step 1 and 2 to analyze how filtering strength affects histogram bin count and complexity, respectively.

2.5.4 Influence of weight types

After defining the best filtering setting, we will analyze how the choice of weight types influences the final complexity results. This will help us understand if certain weight types contribute more significantly to the overall complexity measure.

This will be done by grouping R_{best} in relation to each weight-type combination and calculating the **average** and the **maximum complexity** for each group, then, plotting a bar chart for each metric.

Since we are using combinations symmetrically (each weight type appears the same amount of times in R_{best}), it is not necessary to select a best weight-type combination, like it is done in 2.5.3, because it won't add any bias to the analysis.

2.5.5 Complexity vs Number of parameters

We will analyze how LMC complexity varies with the number of model parameters. This will be done by calculating the **average complexity** for each range of number of parameters, being plotted as a histogram. The number of bins of this plot will be defined using the Freedman-Diaconis rule [54] to adapt to the distribution.

We will look for trends or patterns that may indicate a relationship between model size and complexity.

2.5.6 Complexity vs Number of bins

Similarly to 2.5.5 , we will analyze how LMC complexity varies with the number of histogram bins used in its calculation. This will be done by calculating the **average complexity** for each range of number of bins, being plotted as a histogram. The number of bins of this plot will be defined using the Freedman-Diaconis rule [54] to adapt to the distribution.

We will look for trends or patterns that may indicate a relationship between histogram granularity and complexity.

2.5.7 Complexity vs Benchmark performance

Finally, we will analyze the relationship between LMC complexity and benchmark performance. For each benchmark available in R_{best} , we will create scatter plots with benchmark scores on the x-axis and complexity on the y-axis.

We will perform both linear and free regression analyses (section 2.5.2) to identify trends between complexity and performance. The strength and nature of these relationships will be assessed using Pearson correlation and R^2 values.

As a control, the experiment will be rerun using the number of model parameters instead of LMC complexity. The number of parameters is a known variable that is expected to correlate with benchmark performance according to scaling laws [3]. This will help validate our methodology and provide a baseline for comparison.

We will provide a bar chart summarizing the Pearson correlation coefficient for each benchmark analyzed for both LMC complexity vs benchmark performance and number of parameters vs benchmark performance, so that they can be easily compared. In addition, for each of these plots we will check the result of the concatenation of all benchmarks available to see if a stronger correlation arises from the larger dataset, presented as another bar in the chart.

We will also provide a top 20 list sorted by the absolute value of Pearson correlation coefficients found in the analysis, indicating which benchmark/model/weight-type combinations produced the strongest correlations.

This analysis aims to determine whether higher LMC complexity is associated with better model performance across different benchmarks, in order to validate or refute the hypothesis that complexity correlates with inference capability.

3 Results

3.1 Extraction process

The dataset in section 2.5.1 was built successfully through the process described.

A model with 10 billion parameters took approximately 3.5 hours to process all weight-type combinations and filtering settings using the workstation described in section 2.1. The total parameter count of all models is **652.802.782.352**, taking around **228 hours** (9.5 days) of computation time in total.

The resulting dataset contains **5676 rows**, each representing a unique combination of model, weight-type combination, filtering setting, LMC complexity value, number of histogram bins, and available benchmark results. That was 99 rows short of the expected 5775 rows due to:

- Some unfiltered data models exceeded the maximum number of bins (set to 1 billion) during histogram creation, leading to their exclusion. Increasing the maximum bin count is not possible due to memory constraints and keeping the rows in the dataset capped at 1 billion bins would have introduced bias to the analysis.
- Some numerical values such as count, min, max, mean, std, bin_count, shannon_entropy, desequilibrium, and complexity were reported as NaN or infinite values in certain model and weight-type combinations, which required their exclusion from the dataset. The reasons are unknown, but the main suspects are floating-point precision errors and divisions by zero in some edge cases.

3.2 Filter dimension

Following the methodology described in section 2.5.3, we obtained the plots for average and maximum number of histogram bins per filtering setting across all models and weight-type combinations:

For visualization purposes, unfiltered data is represented as a **40 σ** filtering setting in the plots.

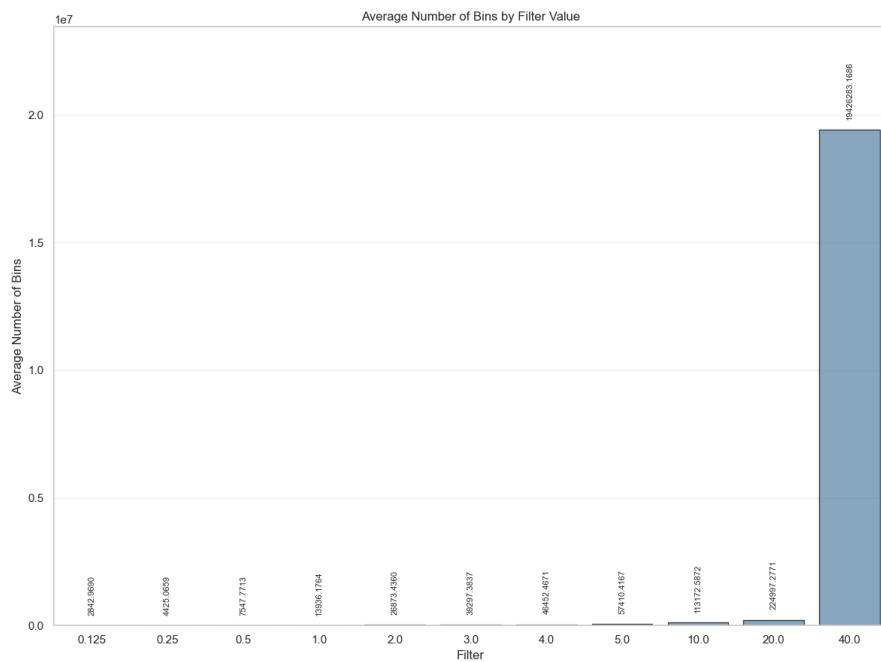


Figure 2: Average number of histogram bins per filtering setting.

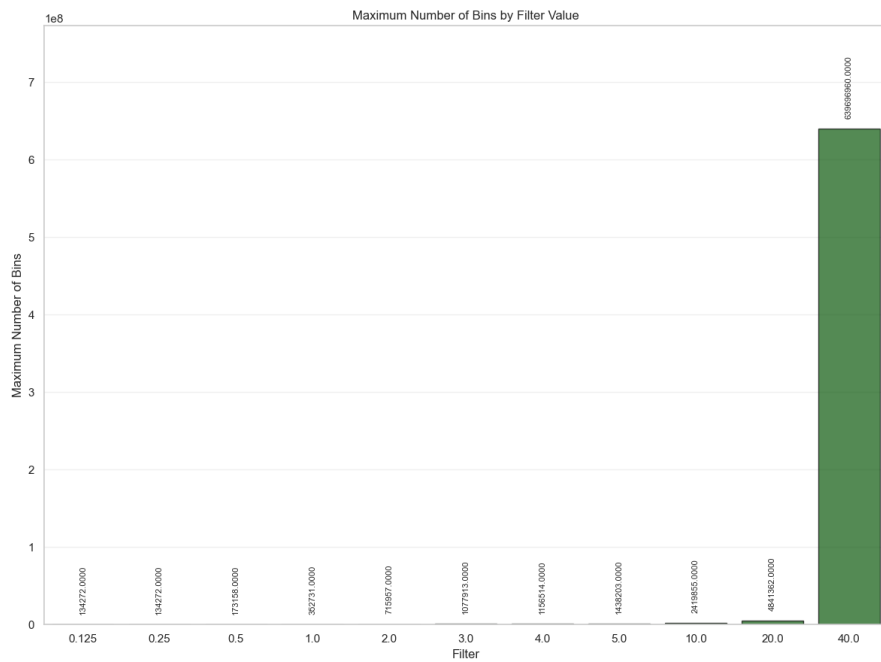


Figure 3: Maximum number of histogram bins per filtering setting.

It is clear that both plots are pretty similar in shape and proportions. There is a big jump downwards from the unfiltered setting (40σ) to the first filtered one (20σ), then a slow and gradual decrease in the number of bins as the filtering becomes more aggressive.

We can understand this behavior more clearly by looking at the regression lines:

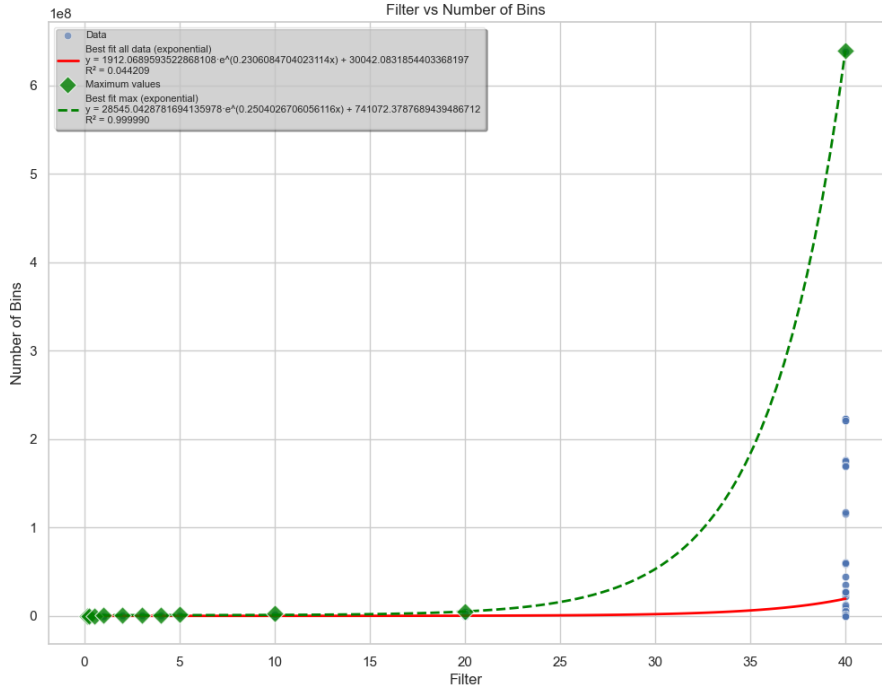


Figure 4: Free regression lines for average and maximum number of histogram bins per filtering setting.

The average bins show a weak fit with $R^2 = 0.044$, indicating high variability. In contrast, the maximum bins demonstrate an exceptional fit with $R^2 = 0.999$. This is expected, as the maximum bins are only one data point per filtering setting, making it easier to fit a curve through them. The fact that both curves follow an **exponential trend**, however, is noteworthy.

The maximum bins (green dashed line) explodes much faster than the average bins (red line) as the filtering becomes less aggressive, meaning that a worst case scenario grows much more rapidly than the average case.

We can also analyze the filtering setting using our second criterion: complexity values. We obtained the following plots for average and maximum LMC complexity values per filtering setting across all models and weight-type combinations:

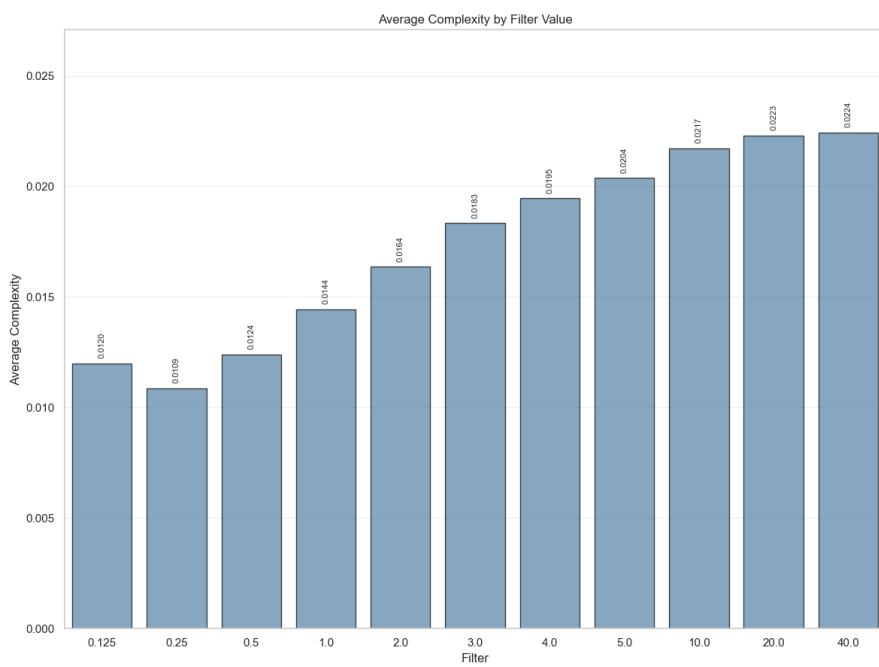


Figure 5: Average number of complexity per filtering setting.

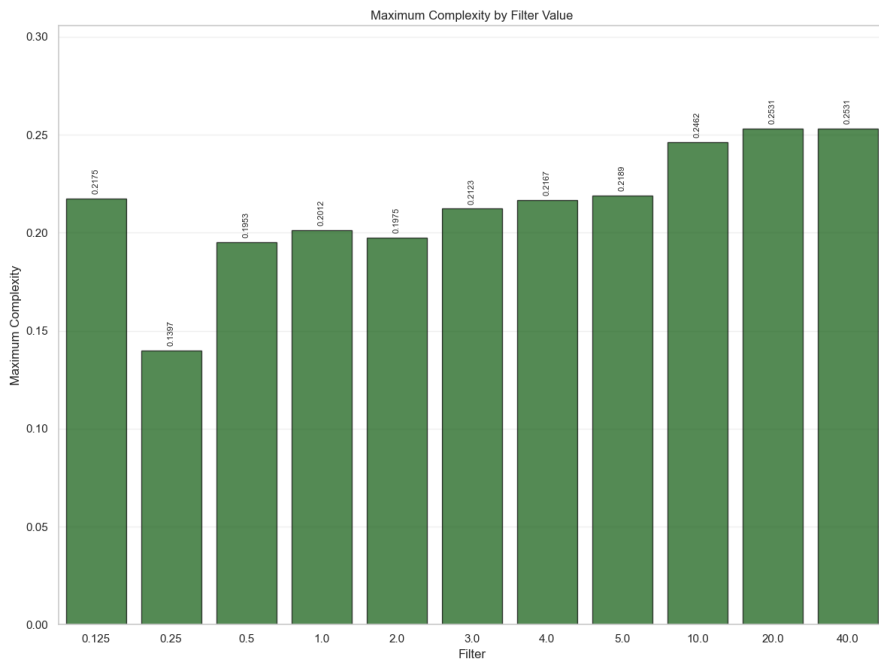


Figure 6: Maximum number of complexity per filtering setting.

We can see that the shape of the plots are similar to each other but follow a different trend compared to the previous figures 2 and 3, more similar to a **logarithmic trend**.

Overall, the maximum values tend to be a bit more flat and unstable, while the average values show a smoother curve. The shapes are not as simple as the previous figures 2 and 3, since it does not follow a monotonous downward trend, we can observe an upward trend from 0.25σ to 0.125σ . For reasons unknown, the 0.25σ bar is a global minimum while we have a spike at 0.125σ .

Complexity values in 10σ and 20σ are almost identical to the unfiltered setting (40σ), followed by a gradual decrease as the filtering becomes more aggressive until reaching the global minimum at 0.25σ .

We can take a look at the regression lines to understand this behavior better:

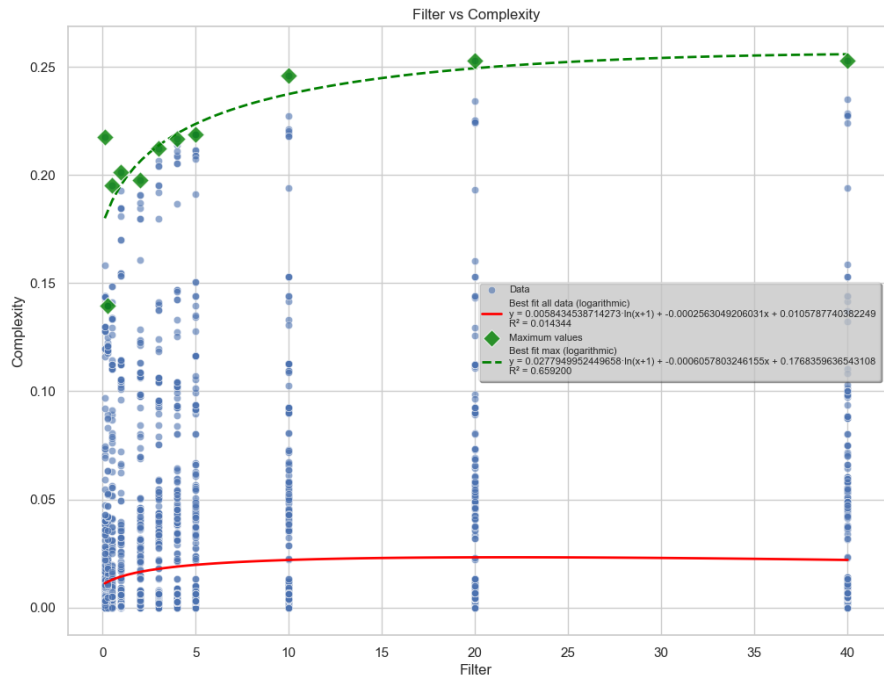


Figure 7: Free regression lines for average and maximum number of complexity per filtering setting.

As expected, both average (red line) and maximum (green dashed line) complexity values follow a **logarithmic trend**, with $R^2 = 0.014$ and $R^2 = 0.659$ respectively. The maximum fit is much better than the average fit due to the same reasons as explained in figure 4, it is, however, much worse than the maximum fit in figure 4, probably due to the unusual spike at 0.125σ .

Both curves show a downward trend as the filtering becomes more aggressive that accelerates the more we approach 0σ , where all the values are removed. This acceleration is faster in the maximum complexity fit.

Analyzing both criteria together, we can conclude that the best filtering setting is 20σ , as it provides a significant reduction in the number of histogram bins while maintaining an almost identical complexity value compared to the unfiltered data.

It looks like that using even less aggressive filtering settings (such as 30σ) could be a better choice, but concluding this would require further experiments with more filtering settings between 20σ and the unfiltered data. More experiments could also be done to understand the intriguing spike in complexity at 0.125σ and how is the behaviour between it and totally filtered data (0σ). However, both of those points are left as future work.

3.3 Weight-type dimension

Following the methodology described in section 2.5.4, we obtained the plots for average and maximum LMC complexity values per weight-type combination across all models using the best filtering setting (20σ):

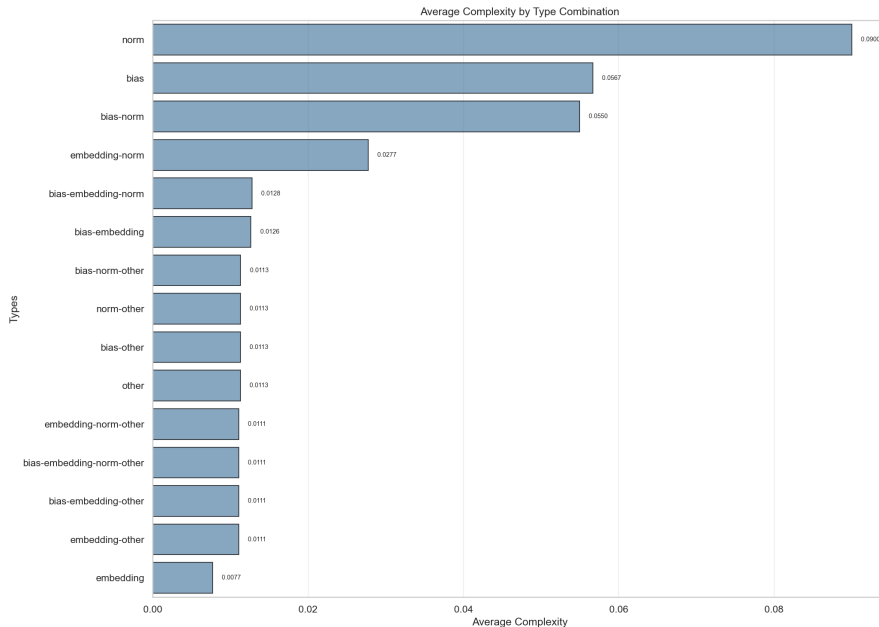


Figure 8: Average complexity per weight-type combination.

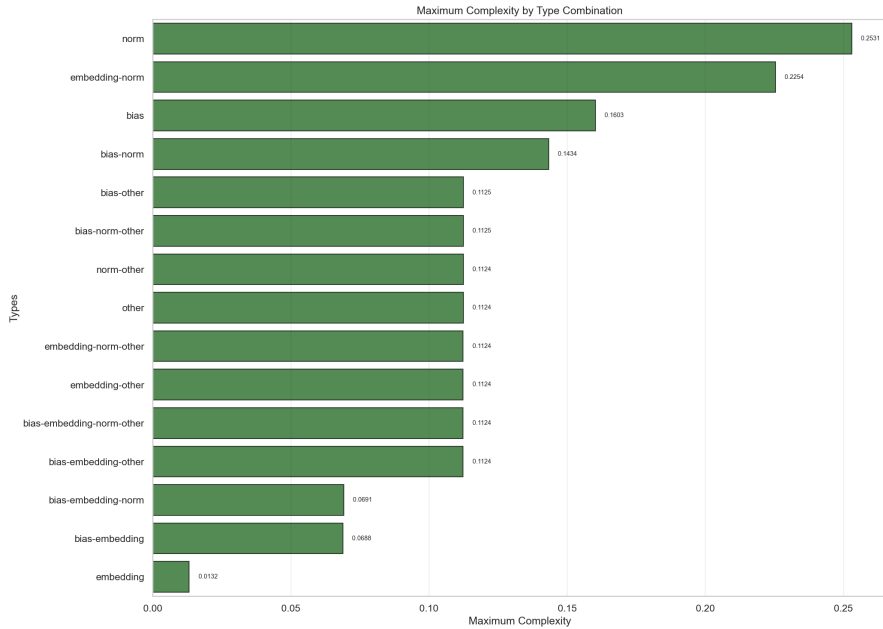


Figure 9: Maximum complexity per weight-type combination.

Again, looking at both plots, we can see that the shapes are similar to each other. In this case we have some variation between the rankings of multiple weight classes (e.g. bias-embedding), which is expected since maximum values can be dominated by outliers. The ranking for single weight types (e.g. bias) is the same across both plots.

Analyzing the multiple weight classes, we can't find a consistent pattern. It is obvious that classes with **other** have similar values since **other** weights are the majority of parameters in a model. It is also interesting to see that **norm** and **bias** individually have higher average complexity values than when combined with each other.

Analyzing the single weight types it is possible to observe that **norm** weights have the highest complexity values, followed by **bias** weights, then **other**, then **embedding**. While norm is responsible for the highest complexity values, embedding are close to zero.

It is unclear why this ranking occurs. It appears to indicate that removing embeddings from a model, like it was done in the scaling laws study [3] won't significantly change its complexity value.

It would be interesting to further investigate if training a model while optimizing the complexity value of certain weight types (e.g. norm) could lead to better performance or generalization. However, this is also left as future work.

3.4 Complexity vs Number of parameters

Following the methodology described in section 2.5.5, we obtained the following plot for average and maximum LMC complexity values against the number of parameters across all weight-type combinations using the best filtering setting (20σ):

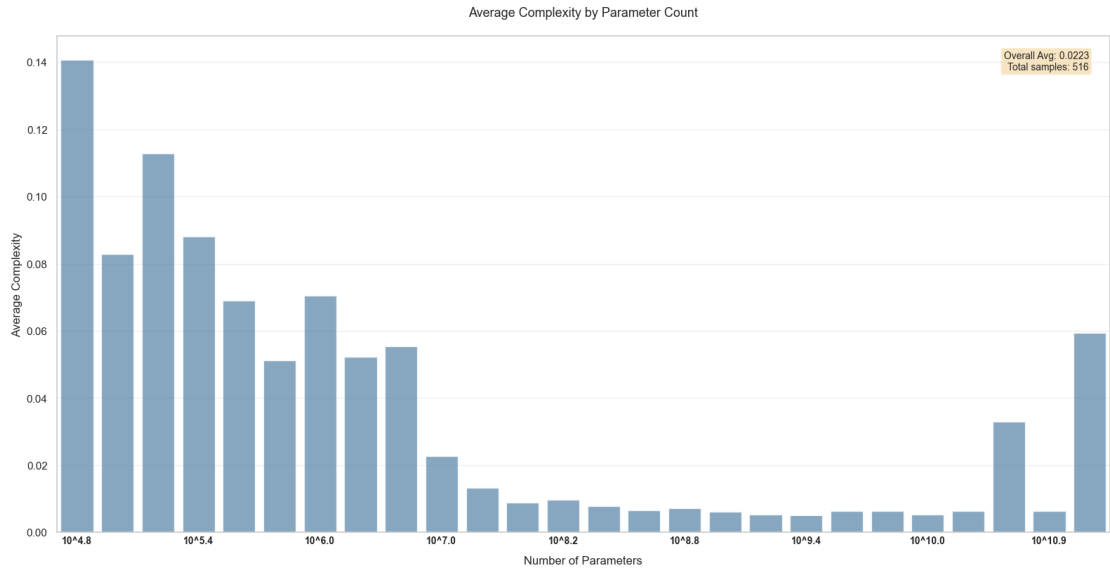


Figure 10: Average complexity vs number of parameters.

A clear trend emerges from the histogram: as the number of parameters increases, the average complexity tends to decrease, with a sudden spike at the end (around $10^{10.9}$ parameters). This indicates that larger models generally exhibit lower complexity values. The spike at the end is, however, unexpected and its causes are unknown.

3.5 Complexity vs Number of bins

Following the methodology described in section 2.5.6, we obtained the following plot for average LMC complexity values against the number of histogram bins across all weight-type combinations using the best filtering setting (20σ):

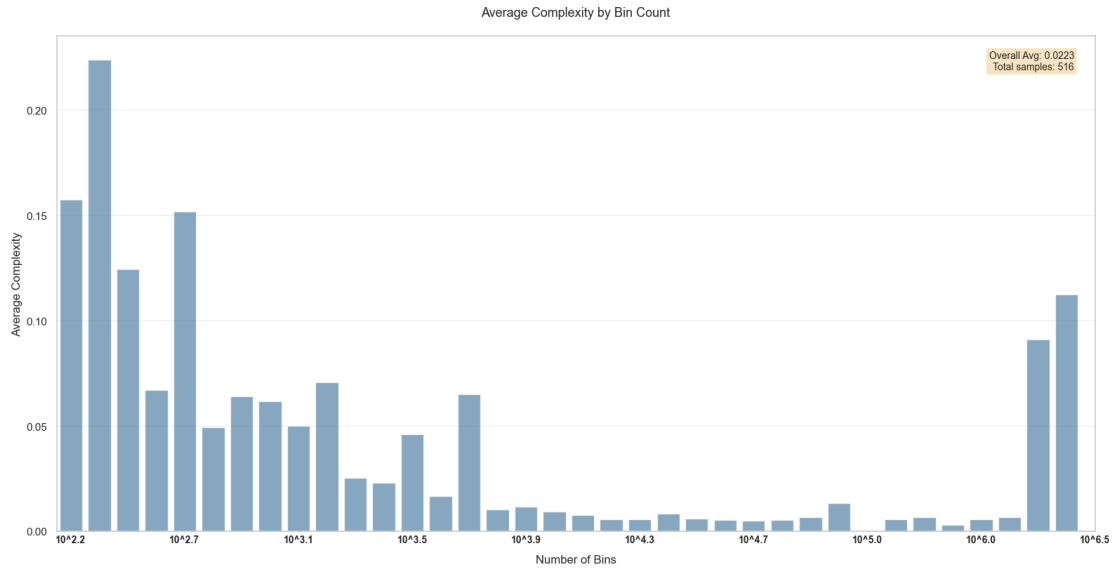


Figure 11: Average complexity vs number of histogram bins.

Again, a clear trend emerges, almost identical to the previous section (3.4). That indicates that there may be a strong correlation between the number of parameters and the number of histogram bins. A possible explanation is that larger models tend to have a wider range of weight values, leading to more histogram bins when using the Freedman-Diaconis choice [54].

3.6 Complexity vs Benchmarks

Following the methodology described in section 2.5.7, first, we made a control plot using a known correlation: parameter count vs benchmark performance. The results are as follows:

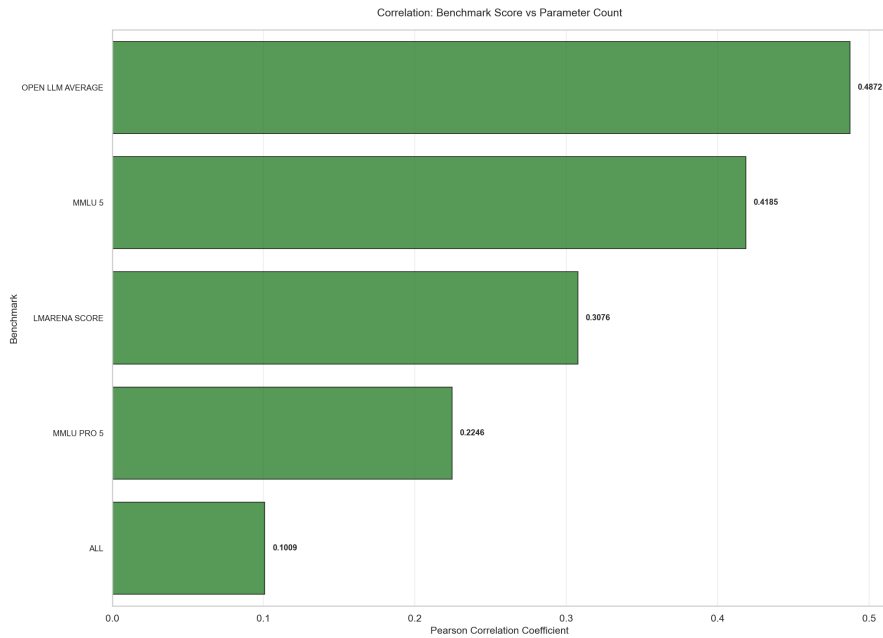


Figure 12: Pearson correlation for parameter count vs benchmark performance.

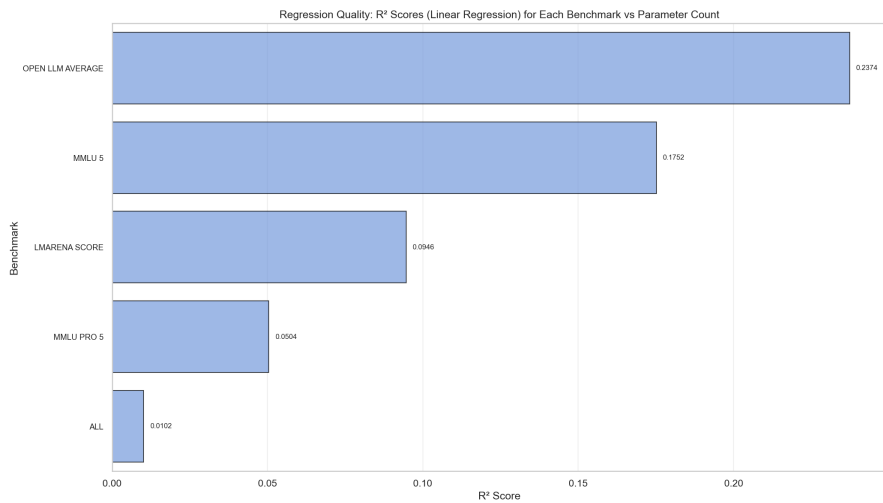


Figure 13: Linear regression R^2 values for parameter count vs benchmark performance.

As expected, all the benchmarks show a positive correlation with parameter count. The linear regression R^2 values are lower, indicating that the relationship is not strictly linear.

Now, we can analyze the actual relationship of interest: LMC complexity vs benchmark performance. The results are as follows:

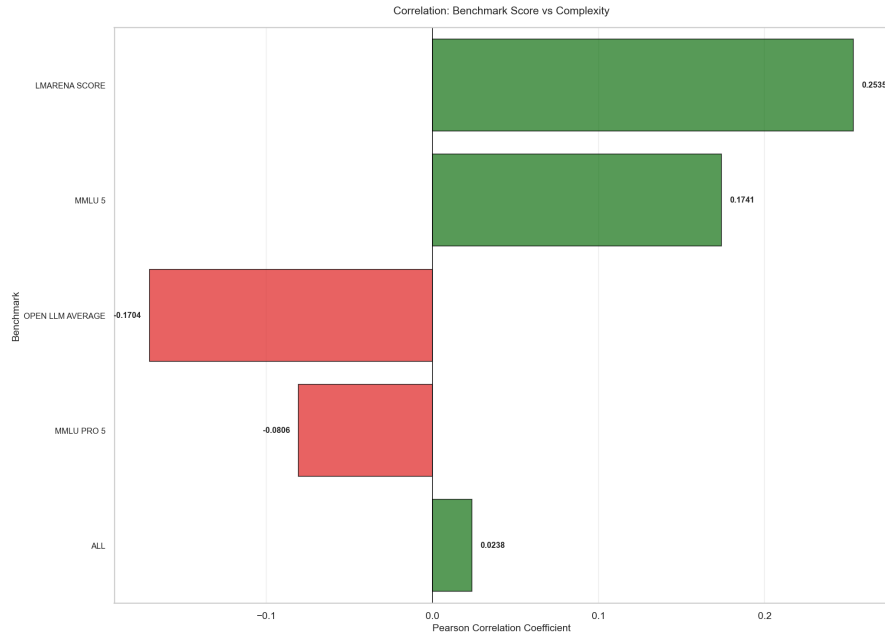


Figure 14: Pearson correlation for Complexity vs benchmark performance.

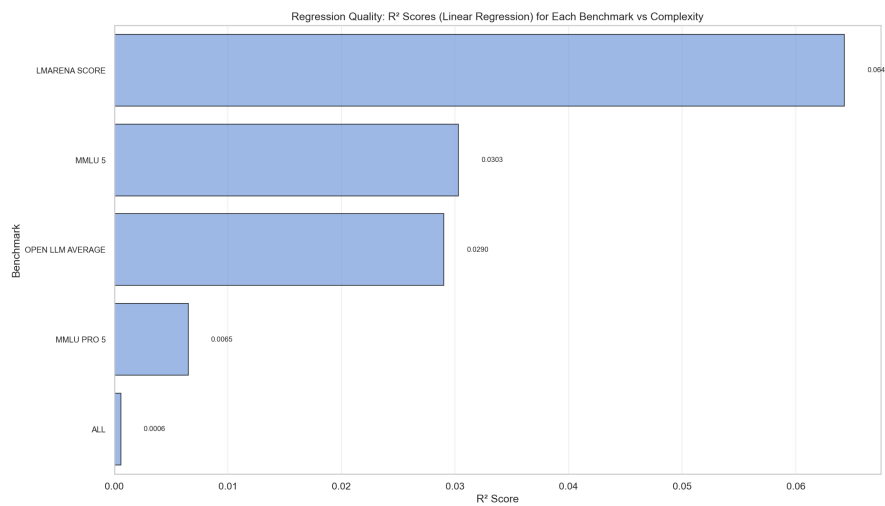


Figure 15: Linear regression R^2 values for complexity vs benchmark performance.

It is immediately clear that results are inconsistent across benchmarks. While

LMArena and **MMLU** show a positive correlation between complexity and performance, **MMLU-Pro** and **OpenLLM** show a negative correlation.

The negative correlations have a smaller absolute value compared to the positive correlations, indicating a bias towards positive correlation. The **all** correlation, formed by analyzing a regression aggregating all data points from all benchmarks, shows a small positive correlation of 0.02, confirming this bias.

The **all** correlation between control and complexity plots is about 5 times smaller (0.10 vs 0.02), indicating that complexity is a much weaker predictor of benchmark performance compared to parameter count. R^2 values are also much smaller in the complexity plot, further confirming the non-linearity of the relationship.

To better understand the shape of the relationship, we can look at the free and linear regression lines for the complexity plots:

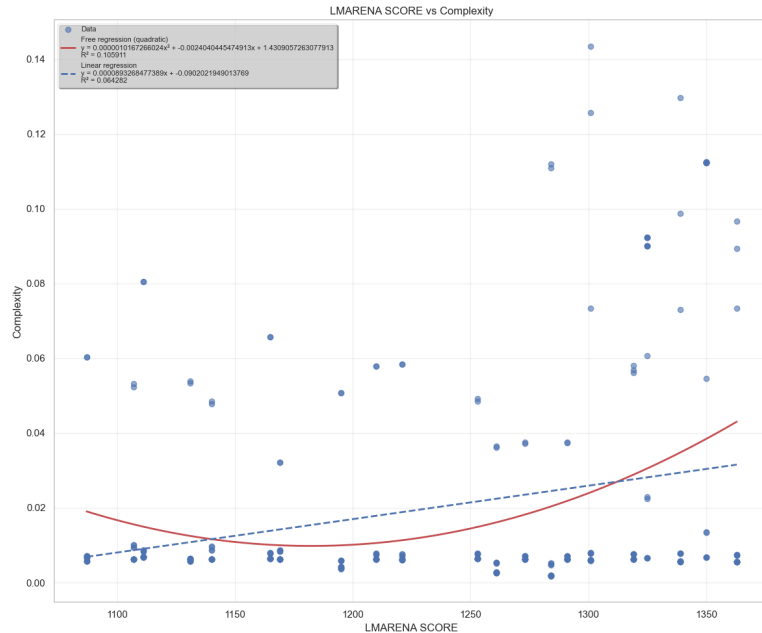


Figure 16: Regression lines for LMC complexity vs LMArena benchmark.

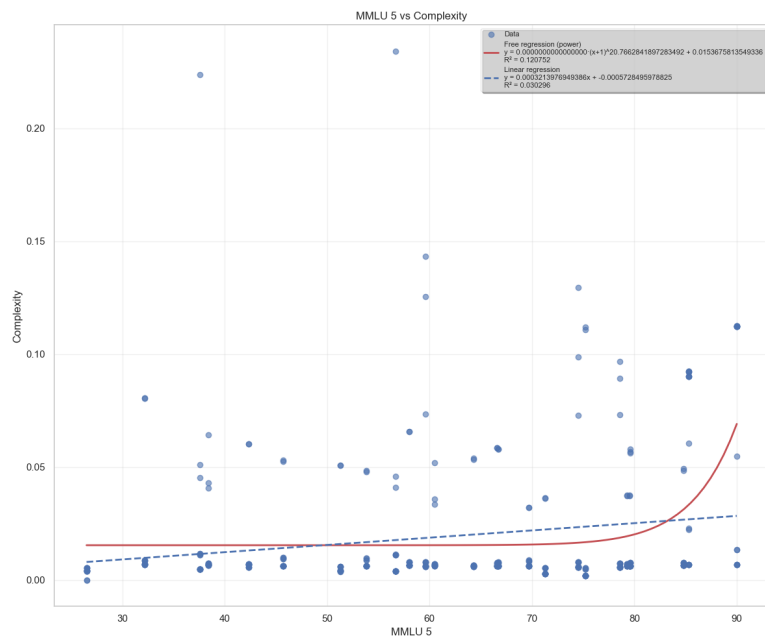


Figure 17: Regression lines for LMC complexity vs MMLU benchmark.

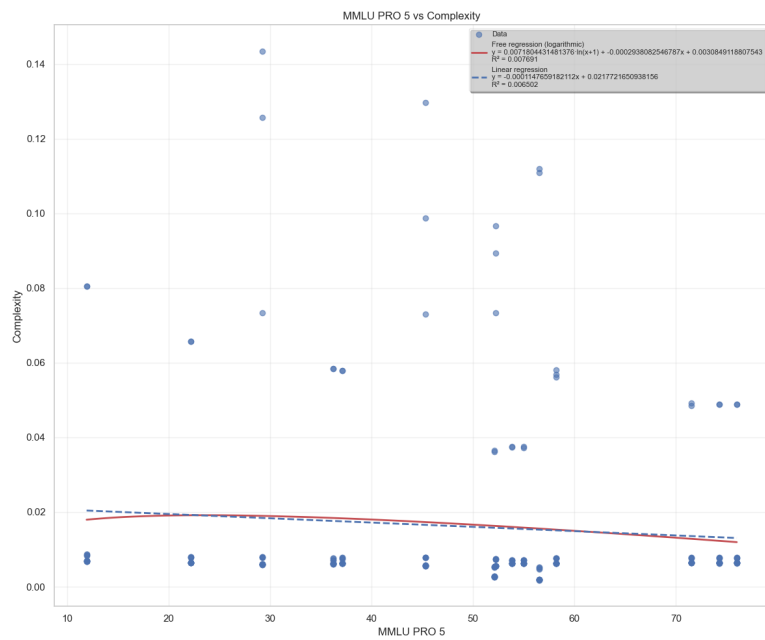


Figure 18: Regression lines for LMC complexity vs MMLU-Pro benchmark.

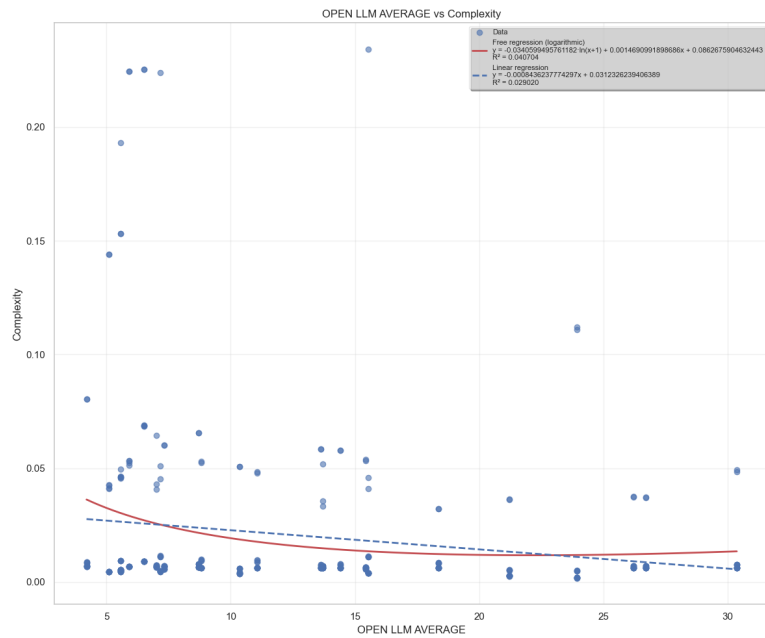


Figure 19: Regression lines for LMC complexity vs OpenLLM benchmark.

We can see that the free regressions can't agree on a common trend since there are **logarithmic**, **exponential** and **quadratic** best fits across the different benchmarks. The benchmarks with negative correlation (MMLU-Pro and OpenLLM) at least agree on having a **logarithmic** trend, but the first one is increasing ($+\ln(x)$) while the second one is decreasing ($-\ln(x)$).

This further confirms that LMC complexity is not a reliable predictor of benchmark performance, as different benchmarks show conflicting relationships with complexity values.

As a bonus, we made a bar plot ranking the top 20 configurations (model + weight-type combination) sorted by highest correlation between LMC complexity and benchmark performance (all benchmarks aggregated):

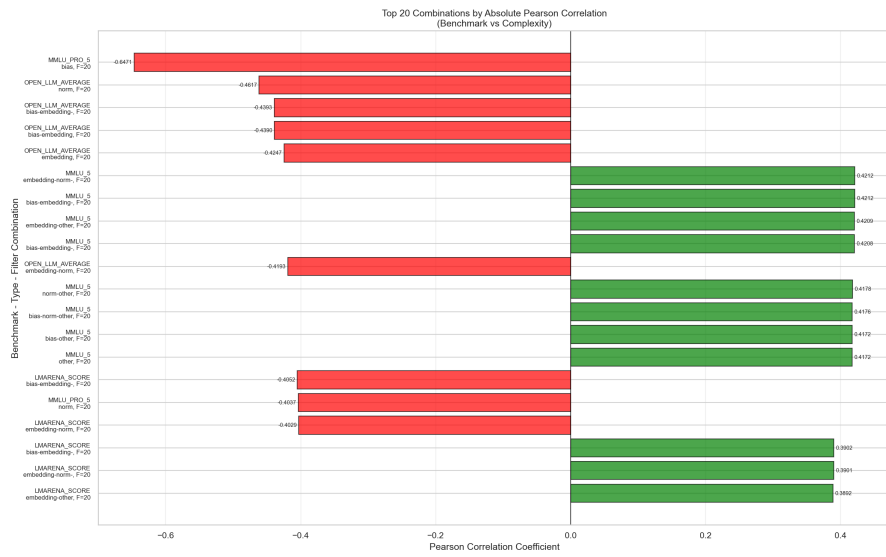


Figure 20: Top 20 configurations by Pearson correlation.

References

- [1] A. Vaswani et al., “Attention is all you need,” *arXiv preprint arXiv:1706.03762*, 2017. [Online]. Available: <https://arxiv.org/abs/1706.03762>
- [2] T. Trust, J. Whalen, and C. Mouza, “Editorial: Chatgpt: Challenges, opportunities, and implications for teacher education,” *Contemporary Issues in Technology and Teacher Education*, vol. 23, no. 1, pp. 1–23, 2023. [Online]. Available: <https://www.learntechlib.org/primary/p/222408/>
- [3] J. Kaplan et al., “Scaling laws for neural language models,” *arXiv preprint arXiv:2001.08361*, 2020. [Online]. Available: <https://arxiv.org/abs/2001.08361>
- [4] T. B. Brown et al., “Language models are few-shot learners,” *arXiv preprint arXiv:2005.14165*, 2020. [Online]. Available: <https://arxiv.org/abs/2005.14165>
- [5] A. Radford, J. Wu, R. Child, D. Luan, D. Amodei, and I. Sutskever, “Language models are unsupervised multitask learners,” 2019. [Online]. Available: https://cdn.openai.com/better-language-models/language_models_are_unsupervised_multitask_learners.pdf
- [6] A. Radford, K. Narasimhan, T. Salimans, and I. Sutskever, “Improving language understanding by generative pre-training,” 2018. [Online]. Available: https://cdn.openai.com/research-covers/language-unsupervised/language_understanding_paper.pdf
- [7] R. Lopez-Ruiz, H. Mancini, and X. Calbet, “A statistical measure of complexity,” *Physics Letters A*, vol. 209, no. 5-6, pp. 321–326, 1995.
- [8] L. O. Murta, *Relationship between model complexity and inference capability*, Personal communication and ongoing research, 2025.
- [9] A. Paszke et al., “Pytorch: An imperative style, high-performance deep learning library,” *arXiv preprint arXiv:1912.01703*, 2019. [Online]. Available: <https://arxiv.org/abs/1912.01703>
- [10] T. Wolf et al., “Huggingface’s transformers: State-of-the-art natural language processing,” *arXiv preprint arXiv:1910.03771*, 2019. [Online]. Available: <https://arxiv.org/abs/1910.03771>
- [11] H. Face, *Huggingface_hub: The hugging face hub python library*, https://huggingface.co/docs/huggingface_hub, 2021.

- [12] P. Virtanen, R. Gommers, T. E. Oliphant, M. Haagerud, A. Reddy, et al., “Scipy 1.0: Fundamental algorithms for scientific computing in python,” *Nature Methods*, vol. 17, pp. 261–272, 2020. DOI: 10.1038/s41592-019-0686-2 [Online]. Available: <https://www.nature.com/articles/s41592-019-0686-2>
- [13] M. L. Waskom, “Seaborn: Statistical data visualization,” *Journal of Open Source Software*, vol. 6, no. 60, p. 3021, 2021. DOI: 10.21105/joss.03021 [Online]. Available: <https://doi.org/10.21105/joss.03021>
- [14] U. R. Pol, P. S. Vadar, and T. T. Moharekar, *Hugging face revolutionizing ai and nlp*, <https://www.researchgate.net/profile/Tejashree-Moharekar/publication/383497950>, 2024.
- [15] *Hugging face – the ai community building the future*, <https://huggingface.co/>, 2024.
- [16] *Ollama – get up and running with large language models locally*, <https://ollama.com/>, 2024.
- [17] *Meta llama 4 scout 17b 16e*, <https://huggingface.co/meta-llama/Llama-4-Scout-17B-16E>, 2024.
- [18] *Meta llama 3.2 3b*, <https://huggingface.co/meta-llama/Llama-3.2-3B>, 2024.
- [19] *Meta llama 3.2 1b*, <https://huggingface.co/meta-llama/Llama-3.2-1B>, 2024.
- [20] *Meta llama 3.1 70b*, <https://huggingface.co/meta-llama/Llama-3.1-70B>, 2024.
- [21] *Meta llama 3.1 8b*, <https://huggingface.co/meta-llama/Llama-3.1-8B>, 2024.
- [22] *Meta llama 3 70b*, <https://huggingface.co/meta-llama/Meta-Llama-3-70B>, 2024.
- [23] *Meta llama 3 8b*, <https://huggingface.co/meta-llama/Meta-Llama-3-8B>, 2024.
- [24] *Meta llama 2 70b hf*, <https://huggingface.co/meta-llama/Llama-2-70b-hf>, 2024.
- [25] *Meta llama 2 13b hf*, <https://huggingface.co/meta-llama/Llama-2-13b-hf>, 2024.
- [26] *Meta llama 2 7b hf*, <https://huggingface.co/meta-llama/Llama-2-7b-hf>, 2024.

- [27] *Google gemma 3 27b pt*, <https://huggingface.co/google/gemma-3-27b-pt>, 2024.
- [28] *Google gemma 3 12b pt*, <https://huggingface.co/google/gemma-3-12b-pt>, 2024.
- [29] *Google gemma 3 4b pt*, <https://huggingface.co/google/gemma-3-4b-pt>, 2024.
- [30] *Google gemma 3 1b pt*, <https://huggingface.co/google/gemma-3-1b-pt>, 2024.
- [31] *Google gemma 2 27b*, <https://huggingface.co/google/gemma-2-27b>, 2024.
- [32] *Google gemma 2 9b*, <https://huggingface.co/google/gemma-2-9b>, 2024.
- [33] *Google gemma 2 2b*, <https://huggingface.co/google/gemma-2-2b>, 2024.
- [34] *Google gemma 7b*, <https://huggingface.co/google/gemma-7b>, 2024.
- [35] *Google gemma 2b*, <https://huggingface.co/google/gemma-2b>, 2024.
- [36] *Google recurrentgemma 9b*, <https://huggingface.co/google/recurrentgemma-9b>, 2024.
- [37] *Google recurrentgemma 2b*, <https://huggingface.co/google/recurrentgemma-2b>, 2024.
- [38] *Microsoft phi 4 mini reasoning*, <https://huggingface.co/microsoft/Phi-4-mini-reasoning>, 2024.
- [39] *Microsoft phi 4 reasoning*, <https://huggingface.co/microsoft/Phi-4-reasoning>, 2024.
- [40] *Microsoft phi 4 reasoning plus*, <https://huggingface.co/microsoft/Phi-4-reasoning-plus>, 2024.
- [41] *Microsoft phi 4*, <https://huggingface.co/microsoft/phi-4>, 2024.
- [42] *Microsoft phi 2*, <https://huggingface.co/microsoft/phi-2>, 2024.
- [43] *Microsoft phi 1.5*, https://huggingface.co/microsoft/phi-1_5, 2024.
- [44] *Microsoft phi 1*, <https://huggingface.co/microsoft/phi-1>, 2024.
- [45] *Openai gpt oss 120b*, <https://huggingface.co/openai/gpt-oss-120b>, 2024.
- [46] *Openai gpt oss 20b*, <https://huggingface.co/openai/gpt-oss-20b>, 2024.
- [47] *Openai gpt-2 xl*, <https://huggingface.co/openai-community/gpt2-xl>, 2024.

- [48] *Openai gpt-2 large*, <https://huggingface.co/openai-community/gpt2-large>, 2024.
- [49] *Openai gpt-2 medium*, <https://huggingface.co/openai-community/gpt2-medium>, 2024.
- [50] *Openai gpt-2*, <https://huggingface.co/openai-community/gpt2>, 2024.
- [51] H. A. Sturges, “The choice of a class interval,” *Journal of the American Statistical Association*, vol. 21, no. 153, pp. 65–66, 1926. [Online]. Available: <https://www.jstor.org/stable/2965501>
- [52] J. Moral De La Rubia, “Rice university rule to determine the number of bins,” *Open Journal of Statistics*, 2024. doi: 10.4236/ojs.2024.141006 [Online]. Available: https://www.scirp.org/pdf/ojs_2024022914191399.pdf
- [53] K. H. Knuth, “Optimal data-based binning for histograms,” *arXiv preprint arXiv:physics/0605197*, 2006. [Online]. Available: <https://arxiv.org/abs/physics/0605197>
- [54] D. Freedman and P. Diaconis, “On the histogram as a density estimator: L_2 theory,” *Zeitschrift für Wahrscheinlichkeitstheorie und Verwandte Gebiete*, vol. 57, pp. 453–476, 1981. [Online]. Available: <https://link.springer.com/content/pdf/10.1007/BF01025868.pdf>
- [55] D. Owen, “How predictable is language model benchmark performance?” *arXiv preprint arXiv:2401.04757*, 2024. [Online]. Available: <https://arxiv.org/abs/2401.04757>
- [56] I. Magar and R. Schwartz, “Data contamination: From memorization to exploitation,” *arXiv preprint arXiv:2203.08242*, 2022. [Online]. Available: <https://arxiv.org/abs/2203.08242>
- [57] D. Hendrycks et al., “Measuring massive multitask language understanding,” *arXiv preprint arXiv:2009.03300*, 2020. [Online]. Available: <https://arxiv.org/abs/2009.03300>
- [58] Y. Wang et al., “Mmlu-pro: A more robust and challenging multi-task language understanding benchmark,” *arXiv preprint arXiv:2406.01574*, 2024. [Online]. Available: <https://arxiv.org/abs/2406.01574>
- [59] A. Myrzakhan, S. M. Bsharat, and Z. Shen, “Open-llm-leaderboard: From multi-choice to open-style questions for llms evaluation, benchmark, and arena,” *arXiv preprint arXiv:2406.07545*, 2024. [Online]. Available: <https://arxiv.org/abs/2406.07545>

- [60] W.-L. Chiang et al., “Chatbot arena: An open platform for evaluating llms by human preference,” *arXiv preprint arXiv:2403.04132*, 2024. [Online]. Available: <https://arxiv.org/abs/2403.04132>
- [61] Y. Li, S. Bubeck, R. Eldan, A. Del Giorno, S. Gunasekar, and Y. T. Lee, “Textbooks are all you need ii: Phi-1.5 technical report,” *arXiv preprint arXiv:2309.05463*, 2023. [Online]. Available: <https://arxiv.org/abs/2309.05463>
- [62] M. Javaheripi and S. Bubeck, *Phi-2: The surprising power of small language models*, <https://www.microsoft.com/en-us/research/blog/phi-2-the-surprising-power-of-small-language-models/>, 2023.
- [63] OpenAI, *Open models*, <https://openai.com/open-models/>, 2024.
- [64] *Llm explorer – compare language models*, <https://llm-explorer.com/>, 2024.
- [65] *Ranked agi*, <https://rankedagi.com/>, 2024.
- [66] G. Cantor, “Beiträge zur begründung der transfiniten mengenlehre,” *Mathematische Annalen*, vol. 46, no. 4, pp. 481–512, 1895. [Online]. Available: <https://webhomes.maths.ed.ac.uk/~v1ranick/papers/cantor1.pdf>
- [67] D. Freedman, R. Pisani, and R. Purves, *Statistics*, 4th. W. W. Norton & Company, 2007.
- [68] T. H. Wonnacott and R. J. Wonnacott, *Introductory Statistics*, English, 5th. Wiley, Jan. 1990, p. 736, ISBN: 978-0471615187.